Interconnection of a two-dimensional array of vertical-cavity surface-emitting lasers to a receiver array by means of a fiber image guide

Tomasz Maj, Andrew G. Kirk, David V. Plant, Joseph F. Ahadian, Clifton G. Fonstad, Kevin L. Lear, Karim Tatah, Matthew S. Robinson, and John A. Trezza

The implementation of a 10-channel parallel optical interconnect consisting of a two-dimensional array of vertical-cavity surface-emitting lasers, a 1.35-m fiber image guide, and a metal–semiconductor–metal receiver array is described. Transmission rates of 250 Mbits/s per channel are demonstrated with an optical cross talk of less than −27 dB and a loss of −3 dB. Coupling issues associated with image guides are analyzed and discussed.

OCIS codes: 060.2360, 200.4650, 140.2010, 110.2350.

1. Introduction

In recent years the development of parallel optical data links has advanced rapidly. They can be used for physically parallel, functionally serial, high-bandwidth links such as intershelf and intercabinet interconnections or in physically and functionally parallel applications such as in CPU to remote memory, a memory bus, or both.[1] Parallel optical data links are being developed for relatively short distances: typically from half a meter to a few hundred meters with per-channel throughputs ranging from 200 to 1000 Mbits/s. At present, commercial optical fiber data links are dominated by fiber ribbons.[2,3] These are suitable for applications that require tens of channels. However, computer bus widths are constantly increasing, and interconnects that possess 128 channels or more may be required in the future. Because of their linear nature, fiber ribbons do not scale well, and two-dimensional (2-D) formats represent a feasible alternative.

Two-dimensional optical data transmission has been achieved with a variety of optical media, including free-space optics, 2-D arrays of optical fibers, and optical fiber image guides (FIG's). Free-space optical interconnects may have applications for short-distance multiple-channel interconnects (of 1 m or less), and they are also used for long-distance single-channel interconnects. However, they are not suitable for multiple-channel long-distance interconnect applications because of diffraction-induced beam spreading and the difficulty of maintaining alignment accuracy. Ordered arrays of optical fibers (with one fiber per transmitter–receiver pair) are potentially useful but present significant challenges in fabrication. The remaining alternative, which is being actively pursued by several researchers, is the optical FIG.[4–10]

A FIG consists of a bundle of many thousands of equally spaced fibers. Flexible FIG's are now commercially available and are widely used in medical imaging applications. Attenuation levels of less than 0.4 dB/m in the 700–1100-nm wavelength range have been measured,[8] and packing densities as high as 0.5×10^6 fibers/cm^2 have been achieved. As an interconnect medium, FIG's represent an oversampled approach in which a single optical channel is transmitted by multiple fibers within the image guide. This approach relaxes alignment tolerances

T. Maj (tmaj@photonics.eee.mcgill.ca), A. G. Kirk, and D. V. Plant are with the Department of Electrical and Computer Engineering, McGill University, 3480 University Street, Montreal, Quebec H3A 2A7, Canada. J. F. Ahadian and C. G. Fonstad are with the Department of Electrical Engineering and Computer Science, Massachusetts Institute of Technology, 77 Massachusetts Avenue, Cambridge, Massachusetts 02139-4307. K. L. Lear is with MicroOptical Devices, Inc., 5601-C Midway Park Place, Northeast, Albuquerque, New Mexico 87109. K. Tatah and M. S. Robinson are with Schott Fiber Optics, Inc., 122 Carlton Street, Southbridge, Massachusetts 01550-1960. J. A. Trezza is with Sanders, Lockheed Martin Company, P.O. Box 868, Mailstop NHQ6-1551, Nashua, New Hampshire 03061-0868.

Received 24 May 1999; revised manuscript received 9 September 1999.

0003-6935/00/050683-07$15.00/0

and ensures that one or more fibers can be damaged without the loss of all power in a channel. Various methods have been used to achieve light coupling into image guides, including the use of microlens arrays, bulk lenses, taper-based coupling, and butt coupling.

Two-dimensional optical data transmission requires the use of 2-D optical emitter arrays. Vertical-cavity surface-emitting lasers (VCSEL's) are a promising low-cost optical emitter technology. For 2-D optical interconnect applications they offer several advantages such as wafer-level testing, circular output beams, compatibility with flip-chip bonding, and ease of fabrication of 2-D arrays. It is predicted that improvements in manufacturing will result in single-mode, high-efficiency, low-threshold, and low-operating-voltage VCSEL's that are compatible with simple drive circuits.[11–13] Such VCSEL's have been demonstrated in several parallel data links.[2,3,14]

To evaluate and demonstrate the suitability of 2-D optical interconnects based on VCSEL's and FIG's, it is necessary to address several issues. These include techniques to align the light emitted from the far end of the image guide with a detector array (many demonstrations to date have used single-channel detectors or CCD cameras), the level of signal uniformity across multiple channels, the total optical power loss in the system, and the level of optical cross talk. In this paper, we attempt to address some of these issues by demonstrating the parallel transmission of optical signals from an 8×8 VCSEL array through a 1.35-m-long image guide. These signals are optically aligned successfully to a metal–semiconductor–metal detector array with a compact and modular optical system. In addition to presenting measurements of optical data rates, loss, and cross talk, we investigate the way in which throughput uniformity is determined by the optical spot size at the image-guide entrance face.

2. Experimental System

The implementation of a unidirectional optical data-transmission system is depicted in Fig. 1. The light emitted from the VCSEL's is imaged onto the entrance face of the image guide with the use of 1:1 imaging optics. The lenses in this optical system are mounted in a custom-designed barrel that is secured within an optomechanical structure on a printed circuit board (PCB). The light emitted from the far end of the image guide is imaged onto the detector array with a similar optical system. The image-guide mount at the receiver permits the image guide to be translated and rotated to align the light emitted from the image guide with the detector array. Aspects of this system and its operation are discussed in detail in Subsection 2.A.

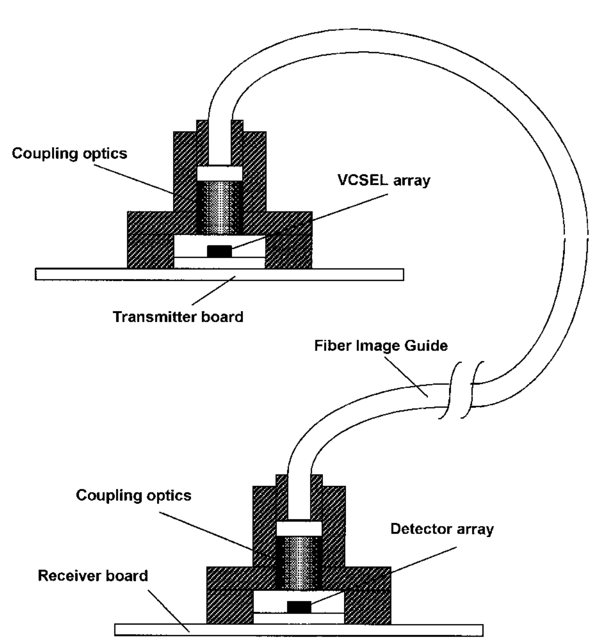

Fig. 1. FIG interconnection system.

A. Vertical-Cavity Surface-Emitting Laser Array and Receiver Module

The VCSEL drivers and the electrical packaging used here were described previously.[14] The VCSEL drivers provide a constant bias current to raise the VCSEL's above threshold. Modulation of the optical intensity is then achieved by voltage modulation. The electrical packaging provides the means to drive 16 independent VCSEL's. The VCSEL chip was therefore wire bonded with 16 out of the 64 lasing devices available in the array. The VCSEL's are on a 250-μm pitch and operate at a wavelength of 840 nm. The beam divergence is approximately 20°, and the output power is between 0.5 and 7 mW.

Figure 2 shows a diagram of the system's transmission module. The VCSEL die was packaged in a 68-pin ceramic-pin-grid array (CPGA) chip carrier. The die was centered in the CPGA and glued to the cavity. A chip thermistor was also inserted into the cavity, and a thermoelectric cooler (peltier) and a heat sink were glued to the back of the CPGA for thermal control.

The receiver array is a monolithic GaAs integrated circuit that combines a 4×4 metal–semiconductor–metal photodetector array on a 250-μm pitch with 70-μm-diameter photodetectors, 1-Gbit/s transimpedance amplifiers, and ECL (emitter–collector logic) output drivers. The receiver die was packaged on a

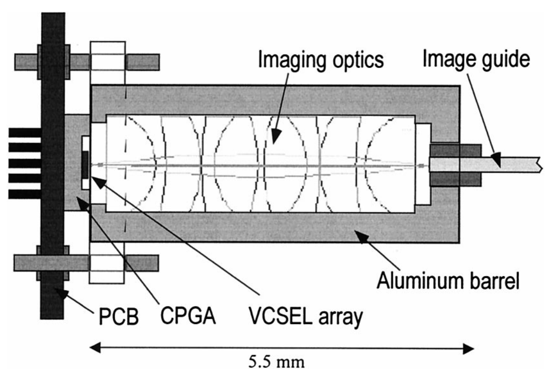

Fig. 2. Transmitter module.

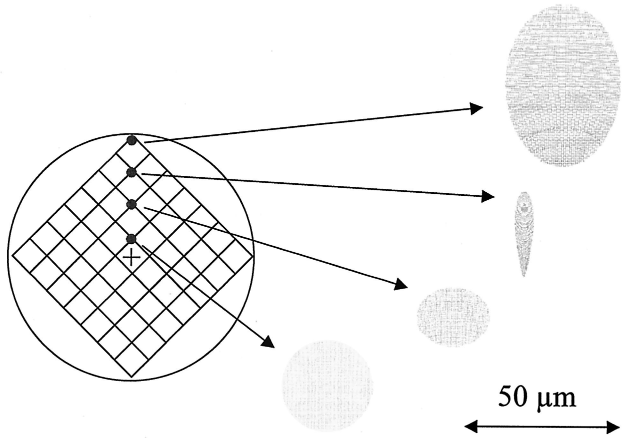

Fig. 3. Simulated spot sizes at the image-guide input face for selected VCSEL's in the 8 × 8 array.

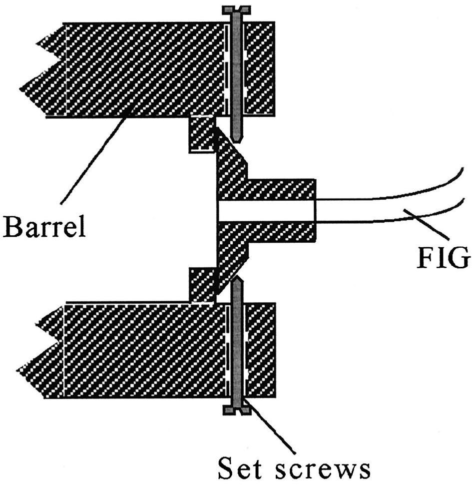

Fig. 4. Receiver receptacle.

PCB that permitted direct high-speed access to the output from all 16 channels.

B. Optical Components and Optomechanics

Imaging optics were required to couple the light emitted from the VCSEL's onto the image guide and from the image guide to the receiver array. This approach was chosen in lieu of butt-coupling the VCSEL directly to the FIG because of the presence of wire bonds at the VCSEL and the receiver chip that would have impeded butt coupling. Complex packaging that permits alignment of the image guide to the detector array would also have been required. Further, the high numerical aperture of the FIG would make it difficult to maintain a spot size of less than 70 μm at the detector plane. A bulk-lens imaging system was selected in favor of a microlens array (i.e., one microlens for each VCSEL) to maintain ease of alignment of the optical system and also because our main intention was to evaluate the performance of the FIG.

The optical system design was constrained by the high divergence of the VCSEL's and of the FIG (requiring an optical system faster than $f/2$), the relatively large field of view required to image the entire VCSEL array (1.75 mm × 1.75 mm), the need to maintain a spot size of less than 70 μm across the image plane, and a desire to keep the imaging system as compact as possible. These criteria limited the number of suitable commercially available lenses.

A telecentric 1:1 optical imaging-system design was used. This design uses two commercially available four-element objective lenses that are optimized for a wavelength of 830 nm. The effective focal length is 6.5 mm, and the numerical aperture is 0.615. The lenses are diffraction limited and corrected for spherical aberration, coma, and astigmatism. Figure 3 shows simulated spot sizes across the plane of the image guide. To optimize the average spot size for transmission, it was necessary to shift the image plane by 0.1 mm. These results suggest that none of the 64 VCSEL's will have a spot size in excess of 50 μm.

For aligning and interconnecting the lenses at the transmission side the lenses were mounted in a custom-designed aluminum barrel, as shown in Fig. 2. The barrel is held in the mounting plate and rests with one end against the CPGA. The FIG is held in a second barrel and is inserted from the other end. This barrel provides a means for rotational alignment of the FIG. A spacer is used to ensure an optimum distance between the FIG and the lens. The components inside the barrel are locked in place with set screws.

The barrel for the receiver was modified slightly to accommodate the alignment of the image guide to the detectors. As shown in Fig. 4, chamfering was added to the FIG barrel so that it could be translated laterally with respect to the receiver array with the aid of set screws. The range of movement is 2 mm, and the positioning accuracy is estimated to be between 10 and 20 μm. Finally, the barrel is held in a mounting plate that itself is attached to the PCB board.

C. Fiber Image Guide

A FIG consists of a coherent bundle of individual step-index fibers. Fiber diameters typically range from 8 to 20 μm, and their relative spatial positions are maintained throughout the bundle.[9] Per central quality area, FIG's can be manufactured with a total of 0.05% gray–dark fibers, which is considered to be acceptable for bundles used in imaging applications and should be sufficient for optical interconnects.

The properties of the 1.35-m image guide used in the system are summarized in Table 1. The cross section of this image guide is hexagonal with a diagonal length of 1.93 mm that does not cover the entire area of the 8 × 8 VCSEL array and prevents the VCSEL's on the edge of the die from being transmitted. Therefore most of the analysis was performed for the central 10 wire-bonded VCSEL's. The fibers at the ends of the image guide are held in a rigid glass

Table 1. Summary of the FIG Parameters

Parameter	Value
Cable diameter	1.93 mm
Length	1.35 m
Pixel count	17,000
Numerical aperture	0.55
Core size	10.0 μm O.D.[a]
Cladding thickness	1.4 μm
Total fiber size	12.7 μm O.D.

[a]O.D., outer diameter.

matrix and protected by a metal jacket. The rest of the guide consists of loose fibers in a plastic sleeve. The image guide is fragile, especially near the interface between the rigid and the loose fibers, and breakage may occur at that point. Figure 5 shows a cross section of the image guide.

Skew and dispersion limit the maximum bandwidth of a communications system. Because every signal in a FIG is transmitted over several cores, skew or multipath dispersion can limit the data rate. Furthermore, a FIG with 10-μm core sizes implies that individual fibers are multimode for 850-nm wavelength light, and modal dispersion will also limit the bandwidth over longer distances. All the optical fibers of a FIG usually are fabricated under the same conditions, and their characteristics are expected to be uniform. Published results[6] suggest that total pulse broadening, including skew and all dispersion sources, is less than 2 ps/m. Transmission rates of several gigabits per second per channel should therefore be achievable over distances of 100 m with these devices.

3. Measurements

In this section, we present measurements of uniformity, loss, data rate, and cross talk for this system.

A. Coupling Uniformity

In such a transmission system it is highly desirable to obtain a uniform power distribution across the receivers. This uniformity simplifies the design of the receiver array because it allows the array to have a common decision level. It also eliminates the need to adjust each channel individually. Optical signal-

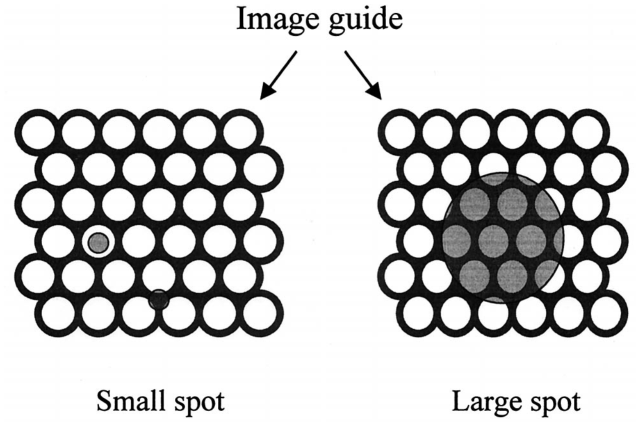

Fig. 6. Illustration of the impact of the spot size on the coupling uniformity.

power uniformity is even more essential when operating receivers in an optically differential configuration.

Nonuniformity of the insertion loss is one potential disadvantage of FIG's. Although the location of the image guide with respect to the VCSEL array and the receiver is known, the energy of a single optical channel is distributed randomly over several cores and the cladding. The optical power coupled into the cladding is diffused or combined into adjacent cores. The power throughput therefore varies as a function of the input spot size and position. If a spot is small almost all of the optical power may be coupled into a single fiber, yielding a low insertion loss. If the center of a spot falls on a cladding area, however, a high coupling loss will be experienced. As illustrated in Fig. 6, one possible solution is to increase the spot size at the image-guide input face. This increase will cause the spot to couple into several fibers and so reduce power variations. However, for maximum parallelism the channels should be closely spaced, so a smaller spot size is desirable to prevent optical cross talk. Thus there is a trade-off between uniformity and channel density as functions of spot size.

Figure 7 shows the spot pattern at the input to the image guide (i.e., after imaging through the transmitter optics). The spot quality is good, and there is no discernible geometric distortion. Figure 8 shows

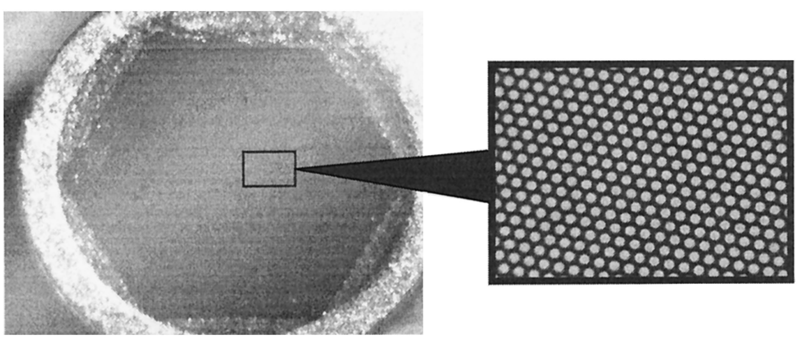

Fig. 5. FIG cross section.

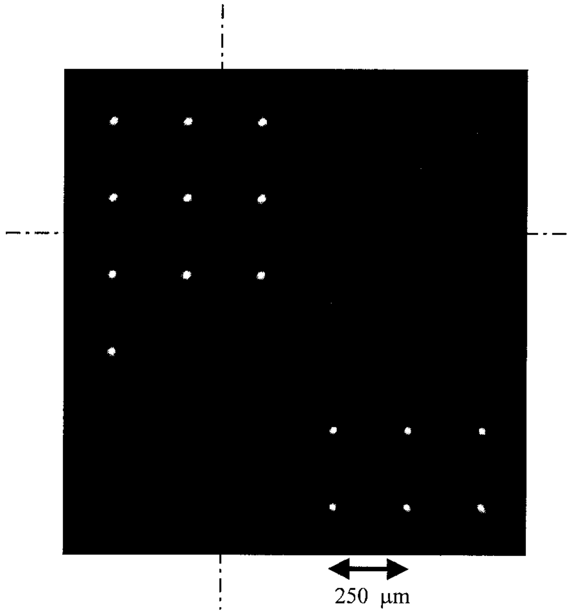

Fig. 7. Spot pattern at the image-guide input face.

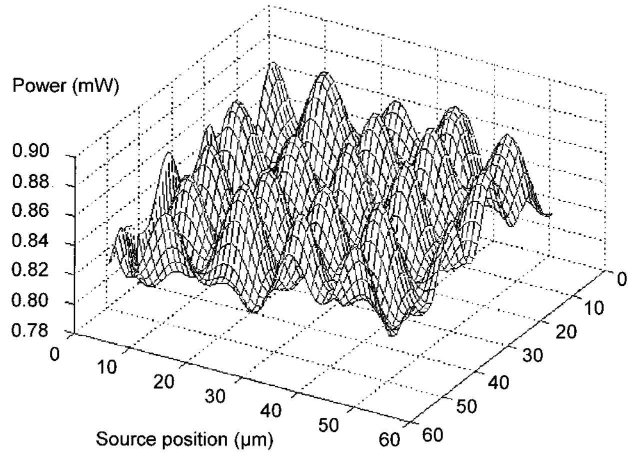

Fig. 9. Throughput variation with respect to the VCSEL–image-guide positions.

the output spot pattern after transmission through the image guide. As expected, each channel has been coupled into several fibers. A calibrated CCD camera was used to measure spot sizes. At the front face of the image guide the average measured spot radius was found to be 15–25 μm. The spot size at the detector is slightly larger and is estimated to be 20–30 μm. These values remain within the constraints imposed by the 35-μm-radius detectors.

For studying throughput uniformity, the image guide was mounted on a motorized *X–Y* stage, and a single VCSEL from the array was operated in cw mode. Two 25-mm lenses in a 4*f* configuration were used to couple the light into the image guide. A power meter recorded the output power as the image guide at the input was translated in two dimensions in steps of 1 μm. The variation in the output power as a 26-μm-radius input beam was scanned across the image guide is shown in Fig. 9. The periodic variation in coupling efficiency is apparent as the spot moves in and out of alignment with a fiber core. For this spot size the variation was ±8%.

Uniformity with respect to the input spot size was determined by the performance of a similar analysis with different input spot radii. Figure 10 shows the dependence of the maximum, the minimum, and the variance of the relative optical output power on the spot size. As expected, the optical power variation decreases as the spot size is increased. The average power remains almost constant. These results suggest that, if uniform coupling losses are required, the input spot size should be as large as possible.

B. Power Throughput

The insertion loss of the system was also measured. A typical loss-distribution analysis is shown in Fig. 11. The two plots represent the best- and the worst-case losses measured over several different channels.

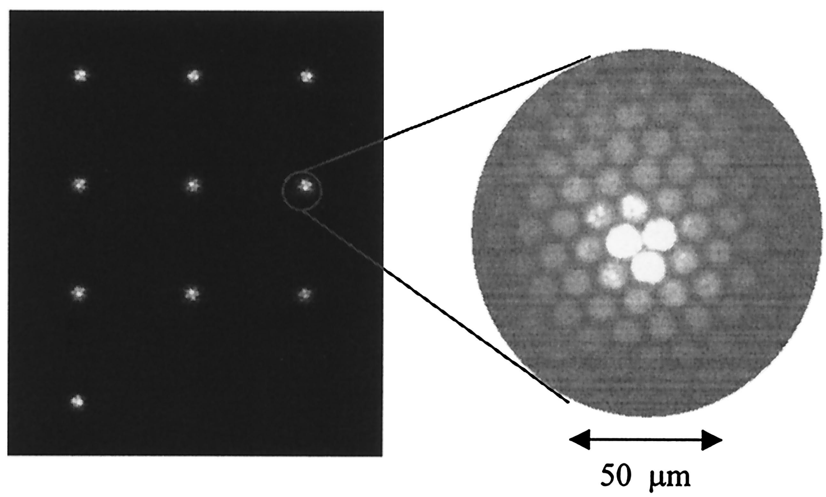

Fig. 8. Spot pattern after transmission through the FIG.

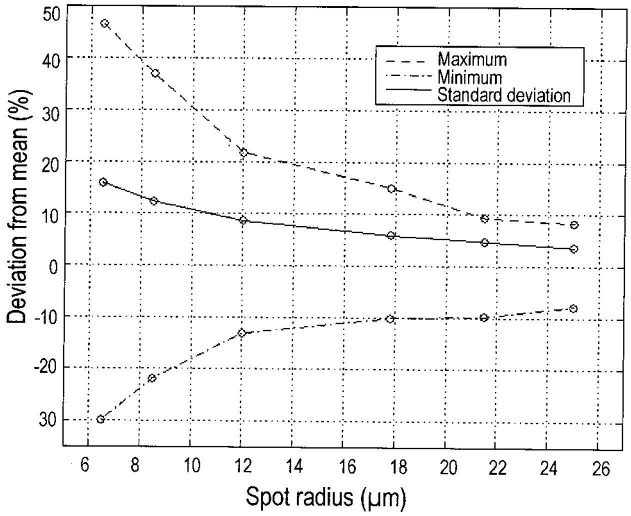

Fig. 10. Coupling uniformity as a function of the spot size at the FIG's input face.

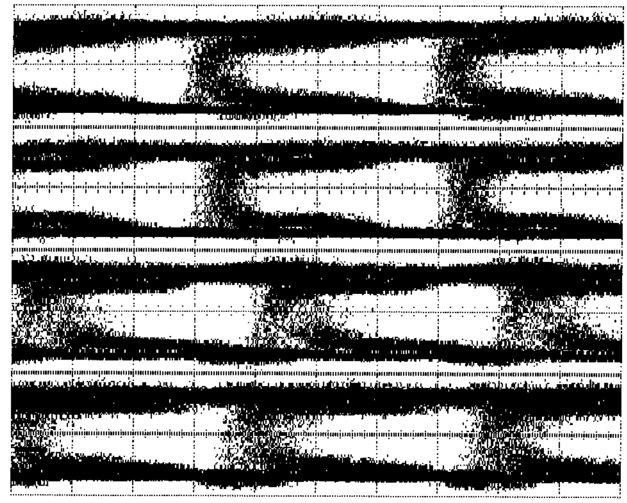

Fig. 12. Eye diagram for four adjacent channels with a 250-Mbit/s modulation. (The time axis represents 1 ns/division.)

The dominant source of loss is in coupling to the image guide. The total loss varied between 3 and 5 dB. Most of the coupling loss can be attributed to the fill ratio of the image guide, which is approximately 0.55. For evaluating the impact of bending loss the image guide was wrapped three times around a 2-mm-diameter metal rod. However, no decrease in output power was measured.

C. Data-Transmission Rates and Optical Cross Talk

By the adjustment of the set screws and the rotation of the image guide in the receiver optomechanics optical signals from all 10 available VCSEL's were aligned simultaneously on the detector array through the image guide. Figure 12 shows a typical eye diagram for four adjacent channels operated at 250 Mbits/s. The maximum bandwidth for multichannel operation was limited by electrical cross talk and noise in the transmitter electronics. A single channel was operated to as high as 1 Gbit/s, confirming that the FIG's can support such data rates.

Optical cross talk incurred through the system was also measured. Cross talk is defined as the ratio of unwanted optical power from an adjacent channel to the desired signal power. Cross talk was measured by the replacement of the receiver array with a 100-μm-diameter pinhole. A single VCSEL was switched on, and the pinhole was translated across the image plane. A power meter was used to measure the optical power transmitted through the pinhole.

Figure 13 shows the variation of the received power with respect to the lateral pinhole position. The center of this curve represents the point at which the pinhole is aligned perfectly with the output beam. Optical cross talk from the closest neighboring chan-

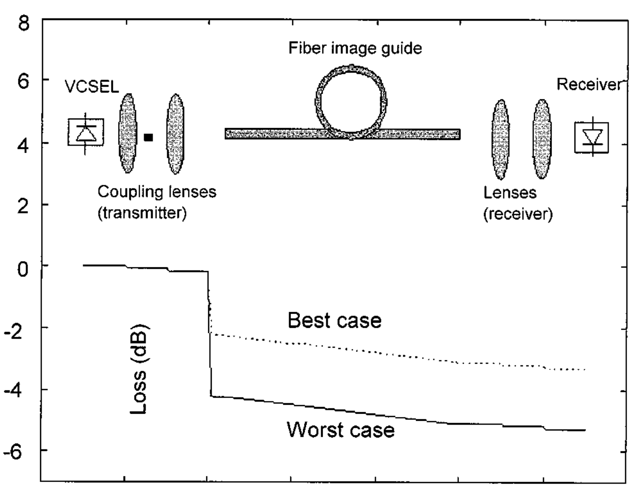

Fig. 11. Insertion-loss distribution.

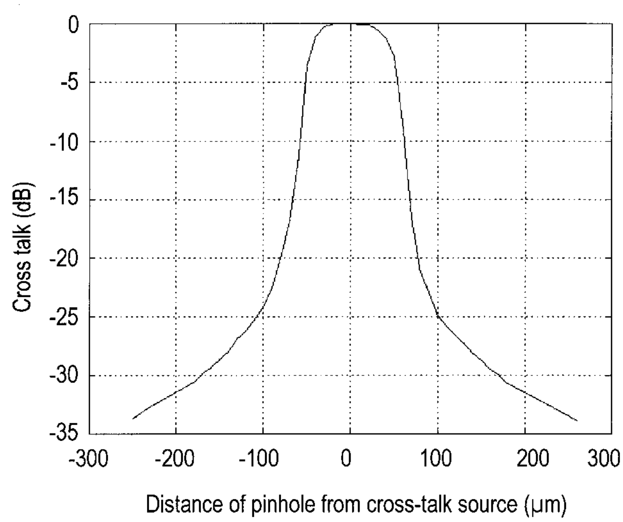

Fig. 13. Cross talk into a 100-μm-diameter aperture as a function of the distance from the cross-talk source.

nel, i.e., the channel 250 μm away from the maximum optical power position, was found to be −33 dB. The total contribution from the four neighboring channels would therefore be less than −27 dB. Similarly, it is possible to conclude that this optical system would support VCSEL's equally well on a 125-μm pitch with a single-channel cross talk of less than −26 dB. This is a conservative measure of cross talk, as the 100-μm detector has twice the area of the 70-μm photodetectors.

4. Conclusion

A parallel optical interconnection based the transmission of light from a 2-D VCSEL array, through a 1.35-m FIG, and onto a detector array has been demonstrated. As many as 10 channels were transmitted simultaneously at 250 Mbits/s with less than −32 dB of optical cross talk per adjacent channel. The input spot size has been found to affect the power uniformity and the coupling efficiency into the FIG. A spot radius of 25 μm was found to yield a 10% power uniformity. A total optical throughput of −3 to −5 dB was measured. Dispersion and skew were not observed over the relatively short length of the FIG used here.

The coupling optics used here consisted of commercially available objective lenses. This optical design does not scale well with increasing array size, and simple butt coupling or some form of micro-optics may be more suitable for future systems. Dedicated connectors are also required to obviate the need for the positioning optomechanics employed here. Bit-error-rate measurements were not carried out for this system and should be performed in the future to determine link performance. It should be noted that, although only 10 channels were transmitted in this system, the number of channels was limited by the number of bonded VCSEL's available. However, this optical system would support at least 36 optical channels on a 250-μm pitch.

The research at McGill University was supported by the Canadian Institute for Telecommunications Research under the National Centres of Excellence Program of the Government of Canada, the National Sciences and Engineering Research Council (NSERC) (OGP0194547), and the Fonds pour la Formation de Chercheurs et l'Aide à la Recherche (FCAR) (NC-1778). Funding for the fabrication of the receiver array was provided by the Optoelectronic Industry Development Association (OIDA).

References

1. J. D. Montgomery and S. Montgomery, "Parallel optical links fill integrated-circuit niches," Laser Focus World **35**(4), 57–59 (1999).
2. W. S. Ishak, K. H. Hahn, B. L. Booth, C. Muheller, A. A. J. Levi, and R. Craig, "Optical interconnects: the POLO project," in *Optoelectronic Interconnects III*, R. T. Chen and H. S. Hinton, eds., Proc. SPIE **2400,** 214–221 (1995).
3. Y. M. Wong, D. J. Muehler, C. C. Faudskar, D. B. Buchholz, M. Fishteyn, J. L. Brandner, W. J. Parzygnat, R. A. Morgan, T. Mullally, R. E. Leibenguth, G. D. Guth, M. W. Facht, K. G. Glogovsky, J. L. Zilko, J. V. Gates, P. J. Anthony, B. H. Tyrone, T. J. Ireland, D. H. Lewis, D. F. Smith, S. F. Nati, D. K. Lewis, D. L. Rogers, H. A. Aispain, S. M. Gowda, S. F. Walker, Y. H. Kwark, R. J. S. Bates, D. M. Kuchta, and J. D. Crow, "Technology development of high density 32-channel 16 Gb/s optical data link for optical interconnection applications for the Optoelectronics Technology Consortium (OETC)," J. Lightwave Technol. **13,** 995–1016 (1995).
4. Y. Li, T. Wang, H. Kosaka, S. Kawai, and K. Kasahara, "Fiber-image-guide–based bit-parallel optical interconnects," Appl. Opt. **35,** 6920–6933 (1996).
5. H. Kasada, M. Kajita, Y. Li, and Y. Sugimoto, "A two-dimensional optical parallel transmission using a vertical-cavity surface-emitting laser array module and an image fiber," IEEE Photon. Technol. Lett. **9,** 253–255 (1997).
6. S. Kawai, Y. Li, and T. Wang, "Skew-free optical interconnections using VCSEL-based fiber image-guides," in *The Sixth Microoptics Conference and the Fourteenth Topical Meeting on Gradient Index Optical Systems*, MOC/GRIN Technical Digest (The Japan Society of Applied Physics, Tokyo, 1997), pp. 78–80.
7. Y. Li, T. Wang, and S. Kawai, "Distributed crossbar interconnects with vertical-cavity surface-emitting laser–angle multiplexing and fiber image guides," Appl. Opt. **37,** 254–263 (1998).
8. K. Tatah, D. Filkins, B. Greiner, and M. Robinson, "Performance measurements of fiber imaging guides and fiber bundles on optical interconnect applications," in *Digest of the Topical Meeting on Optics in Computing* (Optical Society of America, Washington, D.C., 1999), pp. 115–117.
9. D. M. Chiarulli, S. P. Levitan, P. Derr, R. Menon, and N. Wattanapongsakorn, "Multichannel optical interconnections using imaging fiber bundles," in *Digest of the Topical Meeting on Optics in Computing* (Optical Society of America, Washington, D.C., 1999), pp. 112–114.
10. T. Maj, A. Kirk, D. Plant, J. Ahadian, C. Fonstad, K. Lear, K. Tatah, M. Robinson, and J. A. Trezza, "Interconnection of a 2D VCSEL array to a receiver array via a fiber image guide," in *Digest of the Topical Meeting on Optics in Computing* (Optical Society of America, Washington, D.C., 1999), paper PDP3.
11. K. D. Choquette, K. Lear, R. P. Schneider, Jr., K. M. Geib, and H. C. Chui, "Selectively oxidized vertical-cavity lasers," in *Proceedings of the IEEE Lasers and Electro-Optics Society Annual Meeting 1995* (Institute of Electrical and Electronics Engineers, New York, 1995), paper SC1 14.1, pp. 412–413.
12. B. Weigl, M. Grabherr, C. Jung, R. Jäger, G. Reiner, R. Michalzik, D. Sowada, and K. J. Ebeling, "High-performance oxide-confined GaAs VCSEL's," IEEE J. Select. Topics Quantum Electron. **3,** 409–415 (1997).
13. E. M. Strzelecka, D. A. Louderback, B. J. Thibeault, G. B. Thompson, K. Bertilsson, and L. A. Coldren, "Parallel free-space optical interconnect based on arrays of vertical-cavity lasers and detectors with monolithic microlenses," Appl. Opt. **37,** 2911–2821 (1998).
14. D. V. Plant, B. Robertson, H. S. Hinton, M. H. Ayliffe, G. C. Boisset, W. Hsiao, D. Kabal, N. H. Kim, Y. S. Liu, M. R. Otazo, D. Pavlasek, A. Z. Shang, J. Simons, K. Song, D. A. Thompson, and W. M. Robertson, "4 × 4 vertical-cavity surface-emitting laser (VCSEL) and metal–semiconductor–metal (MSM) optical backplane demonstrator system," Appl. Opt. **35,** 6365–6368 (1996).